Application of Remote Wind-Forced Coastal Trapped Wave Theory to the Oregon and Washington Coasts[1]

DAVID S. BATTISTI[2] AND BARBARA M. HICKEY[3]

University of Washington, Seattle, WA 98195

(Manuscript received 13 December 1983, in final form 21 February 1984)

ABSTRACT

The theory of coastal trapped waves generated by remote wind forcing (Clarke) is used to calculate coastal subsurface pressure (SSP) and longshore velocity along the Oregon and Washington coasts for three two-month periods: summer of 1972, summer of 1978 and winter of 1977. The response in SSP and longshore velocity is assumed to be dominated by the mode one wave. In every case, coherence squared between observed and modeled SSP is significant at the 95% level over the entire low frequency band ($\leq$0.2 cpd) with an average phase difference less than $\pm 30°$. Greater than 80% of the variance in coastal SSP is accounted for by the mode one coastal trapped wave (CTW). The SSP response off Washington and Oregon during summer is primarily ($\sim$35% of the variance) a result of wind forcing between San Francisco and Cape Mendocino, California. Wind stress in this region during summer is significantly larger than that off Oregon and Washington at low frequencies so that the CTW generated off California propagates northward with only minimal input from the local wind field. The local contribution to SSP off Oregon and Washington during summer is relatively small (<15%). The response during winter, on the other hand, is dominated by local wind stress, local winds being much more energetic than those to the south. Comparison between modeled and observed longshore velocity shows that at low frequencies a significant portion of the variance in longshore velocity on the Pacific Northwest shelf is also accounted for by the mode one wind forced CTW.

1. Introduction

Observational evidence for the presence of coastal trapped waves on the Washington and Oregon continental shelf has been presented by numerous investigators over the last few years (Cutchin and Smith, 1973); Mooers and Smith, 1968; Kundu and Allen, 1976; Huyer *et al.*, 1975; Wang and Mooers, 1977; Hseuh and Lee, 1978; Hsieh, 1982; Hickey, 1984). This evidence has been derived primarily through examination of the spatial coherence of the coastal subsurface pressure (SSP) and longshore velocity fields using a variety of standard analysis methods on various data sets. The general results of these studies indicate that in the Pacific Northwest, SSP fluctuations at frequencies < 0.3 cpd during summer are consistent with some of the properties of a freely propagating mode one coastal trapped wave; specifically, at these frequencies SSP is highly coherent over large longshore scales (>400 km), with phase lags suggestive of the first mode coastal trapped wave. These studies consistently find a longshore velocity field which is quasi-barotropic (depth-independent) at low frequencies over the middle and outer shelf, with an amplitude that decays offshore. Depending on the frequency band of interest, location of the current meter and the time (season) of observation, the longshore current fluctuations have been attributed to either freely propagating coastal trapped waves (modes one, two and three), or a local response to wind forcing over irregular coastal topography (bathymetry or coastline shape).

If the coastal subsurface pressure fluctuations off the Pacific Northwest are best described by freely propagating coastal trapped waves, the longshore wind stress is the most obvious generator of these waves, as first noted by Adams and Buchwald (1969). Gill and Schumann (1974) showed that for a purely barotropic ocean these coastal trapped waves satisfy a forced, first-order wave equation. This theory was expanded by Gill and Clarke (1974) and Clarke (1977) to include the effects of both topography and stratification. Clarke showed that for a five week period in summer 1972, the observed coastal subsurface pressure field at frequencies < 0.25 cpd off central Oregon was significantly coherent with that predicted by the mode one wind-forced coastal trapped wave theory.

The purpose of this study is to determine quantitatively to what extent the subsurface pressure and longshore velocity fields in the Pacific Northwest can be accounted for by a wind-forced coastal trapped wave response. Following the theory of Clarke (1977), the pressure and velocity fields are calculated for various locations off Oregon and Washington for two month

[1] Contribution No. 1380 from the School of Oceanography, University of Washington.

[2] Department of Atmospheric Sciences.

[3] School of Oceanography.

time periods in three different years (two summers and one winter). These particular periods have been discussed in detail by Hickey (1984), who shows that in each of these periods the fluctuating large-scale longshore pressure gradient makes significant contributions to the longshore momentum balance, consistent with wave-like dynamics. In the present paper, the contribution of the mode one coastal trapped wave to the observed variance in SSP and longshore velocity in the most energetic frequency band resolved (0.1–0.3 cpd) is quantified by direct comparison of modeled and observed pressure and velocity data. Additionally, the source of significant variance in coastal SSP and midshelf longshore velocity off the Pacific Northwest due to coastal longshore wind stress is identified and the spatial variation of this source is examined on a seasonal time scale.

2. The coastal trapped wave model

a. Free coastal trapped wave model

The coastal trapped free wave has been discussed by Allen (1975), Wang and Mooers (1977), Huthnance (1978), Clarke (1977) and Brink (1982a). To calculate the offshore-vertical structure and dispersion relationship of a free coastal trapped wave, consider a linear, inviscid ocean under constant rotation where the density stratification is horizontally uniform and topography varies only in the offshore direction. Under these conditions the equations of motion are

$$u_t - fv = -P_x/\rho_0, \tag{2.1}$$

$$v_t + fu = -P_y/\rho_0, \tag{2.2}$$

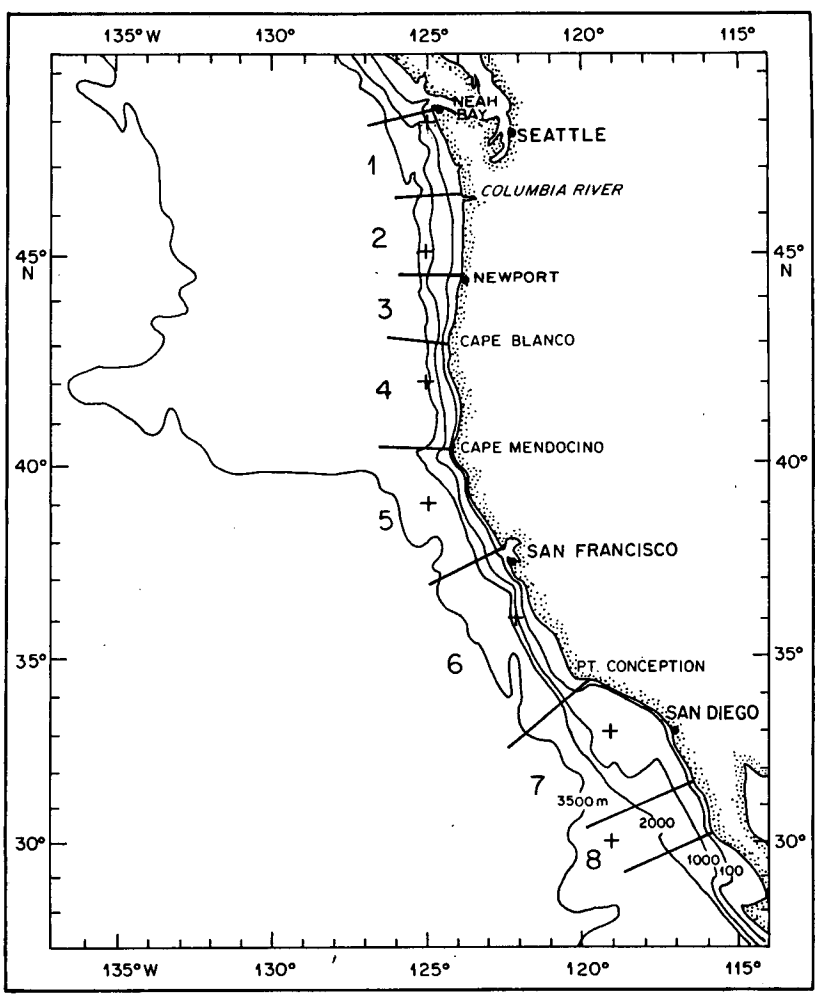

FIG. 1. A map of the west coast of the United States. Selected depth contours have been superimposed to indicate the location of the shelf break and the onshore–offshore bathymetric structure. The segments used in the forced coastal trapped wave model are marked with lines emanating from the coast. Bakun wind stress grid points are indicated by plus signs.

TABLE 1. Description of the data used to calculate the forced coastal trapped hybrid waves and to contrast the forced wave response to that observed. Abbreviations UW, OSU indicate the University of Washington and Oregon State University, respectively.

Year	Meter ID	Data type	Location (lat., long.)	Starting date and length of record used (days)	Source
1972 1977 1978	—	Wind stress	30°N to 51°N, in 3° increments	July 21 (56) Jan 12 (56) Aug 15 (56)	Bakun
1981	—	Density	Oregon, California	—	OSU Report Nos. 93, 96, 99
1975	—	Density	Oregon, Washington	—	UW Report No. 86
1978	ELE, 92 m	Longshore velocity	45°20.1'N, 124°08.8'W	August 15 (56)	
1972	NH20, 50 m	Longshore velocity	44°38.6'N, 124°31.5'W	July 21 (56)	OSU
	MS, 20, 50, 66, 71 m		46°25.0'N, 124°20.0'W	July 21 (56)	
	OS, 20, 30, 55, 110, 160 m		46°50.0'N, 124°50.0'W	July 21 (56)	
	S6, 192, 323, 585 m		46°47.5'N, 124°56.9'W	July 21 (56)	
	S8, 60, 247, 433, 619, 805		46°45.8'N, 125°08.9'W	July 21 (56)	
	S11, 60, 265, 881, 1086 m		46°43.2'N, 125°17.3'W	July 24 (14–22)	
1977	80 m	Longshore velocity	46°49.5'N, 124°32.5'W	Jan 12 (56)	
1972 1977 1978		Subsurface pressure			Hickey (1984)

$$P_z = -g\rho, \tag{2.3}$$

$$u_x + v_y + w_z = 0, \tag{2.4}$$

$$\rho_t = -w\rho_{0z}, \tag{2.5}$$

where u, v and w are the onshore–offshore, longshore and vertical velocities in the x, y, z directions. The coordinates x and y are chosen to be positive onshore and northward, respectively, and z is positive upward. The density perturbation from the rest state $\rho_0(z)$ is $\rho(y, z, t)$. In these equations P is the perturbation pressure, f the Coriolis parameter and g the acceleration due to gravity. Subscripts x, y, z and t denote partial differentiation. Equations (2.1)–(2.5) can be reduced to one equation for the perturbation pressure P

$$P_{xxt} + P_{yyt} + (f^2 + \partial_{tt})(P_z/N^2)_{zt} = 0, \tag{2.6}$$

where $N^2(z) = -g\rho_0^{-1}\rho_{0z}$ is the square of the Brunt-Väisälä frequency. The boundary conditions are

$$(f^2 + \partial_{tt})P_{zt} + N^2h_x(P_{xt} + fP_y) = 0 \quad \text{at} \quad z = -h(x), \tag{2.7}$$

$$P_{zt} + g^{-1}N^2P_t = 0 \quad \text{at} \quad z = 0, \tag{2.8}$$

$$P_{xt} + fP_y = 0 \quad \text{at} \quad x = 0, \tag{2.9}$$

$$P \to 0 \quad \text{as} \quad x \to -\infty. \tag{2.10}$$

Eqs. (2.7) and (2.9) express the conditions of no normal flow through the bottom [$z = -h(x)$] and coast ($x = 0$), and (2.8) is the free surface condition. The final condition (2.10) requires the response to be coastally trapped.

Assuming a response of the form

$$P = \hat{P}(x, z)\exp[i(ly - \omega t)], \tag{2.11}$$

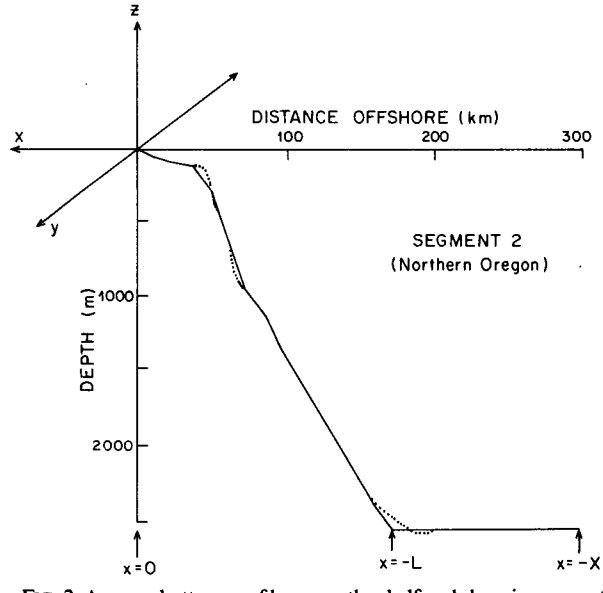

FIG. 2. Average bottom profile across the shelf and slope in segment 2, off northern Oregon (dotted line). The coordinate system superimposed is that used in the text, with $x = 0$ at the coast (x negative offshore). The approximation to the bottom profile used in modeling the free coastal trapped waves is indicated by the solid lines, with $x = -X, -L$ chosen as prescribed by Brink (1982a).

where l is the longshore wavenumber and ω is the frequency, Eqs. (2.6)–(2.10) reduce to a two-dimensional eigenvalue problem. To solve this set of equations for a realistic stratification $N(z)$ and topography $h(x)$, the authors used the numerical wave model developed and generously supplied by Dr. Kenneth Brink. The details of this model are discussed elsewhere (Brink, 1982a,b) and will not be repeated here. The problem is solved on a stretched grid (17 points in the vertical and 25 in the horizontal to enhance resolution in shallow areas) by resonance iteration for ω at a given wavenumber l. This model has been used extensively off Oregon and Peru (Brink, 1982a) and in the Gulf of Guinea (Clarke and Battisti, 1983) with good results.

In order to calculate the free wave response along the coast, the coastal zone was divided into segments such that within each segment, longshore topography, rotation and stratification were essentially uniform (Fig. 1). The density field along each transect was horizontally averaged at depth increments of 10 m to a depth of 300 m, and an exponential fit for $N^2(z)$ was assumed from 300 m to the bottom at $z = -h$. Sources of the density data are listed in Table 1. Typical bottom topography and density profiles [given as $N^2(z)$] for the Pacific Northwest are illustrated in Figs. 2 and 3, respectively.

The dispersion curves for the first three modes for northern Oregon are shown in Fig. 4; the offshore-

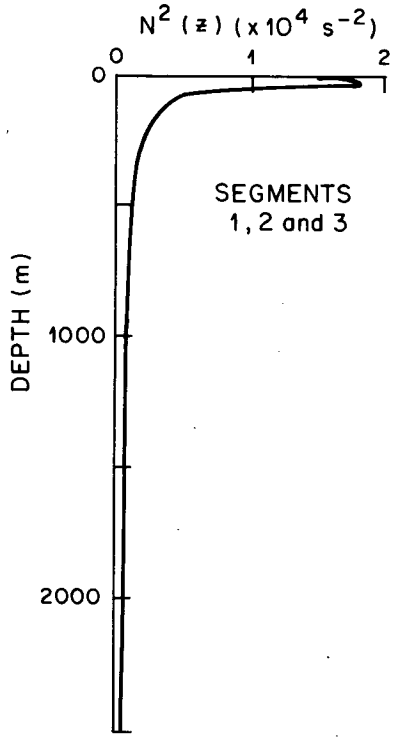

FIG. 3. The offshore-averaged profile of Brunt-Väisälä frequency squared for segments 1, 2 and 3 of Fig. 1.

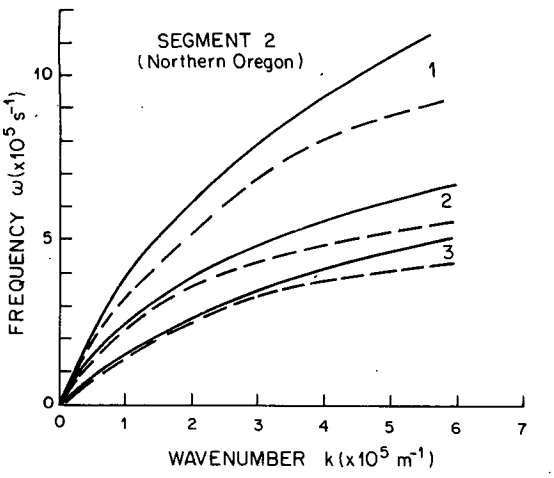

FIG. 4. Dispersion curves for the first three hybrid coastal trapped wave modes for segment 2 (northern Oregon). The solid curves were calculated using the realistic topography and stratification shown in Figs. 2 and 3, respectively. The dashed curves were calculated using weak near-surface stratification profiles that might result from vigorous storm mixing. The mode number is indicated on the right side of each pair of curves.

vertical structure for modes one and two is depicted in Fig. 5. The nondispersive phase speeds for modes one and two are 3.8 m s^{-1} and 2.3 m s^{-1}, respectively, off northern Oregon. Figure 5 illustrates that the response in longshore velocity is essentially barotropic, consistent with the results of Brink (1982a) for a high latitude long wave.

To determine qualitatively the sensitivity of the model wave speed and spatial structure to stratification changes, cases were run with both a strongly stratified upper water column and an extremely weakly stratified upper water column. These cases might represent the density structure near the Columbia River and that during an energetic storm, respectively. In the "well mixed" case, $N^2(z)$ was decreased by a factor of 10 in the first 100 meters of the water column. The results demonstrated that the cross-shelf structures of modes one and two were relatively unaffected by changes in surface stratification (not shown). The phase speed in the nondispersive frequency range is also essentially unaffected by such changes in the near-surface stratification (<5%) (e.g., Fig. 4). However, the phase speed at higher frequencies is a function of stratification: weaker upper water column stratification is associated with slower phase speeds and more pronounced flattening of the dispersion curves. Note that these curves, calculated with realistic stratification and bottom topography, do not "turn over" as do dispersion curves calculated for the purely barotropic case (Cutchin and Smith, 1973). Thus, free coastal trapped wave energy can propagate only northward along the Oregon and Washington coasts.

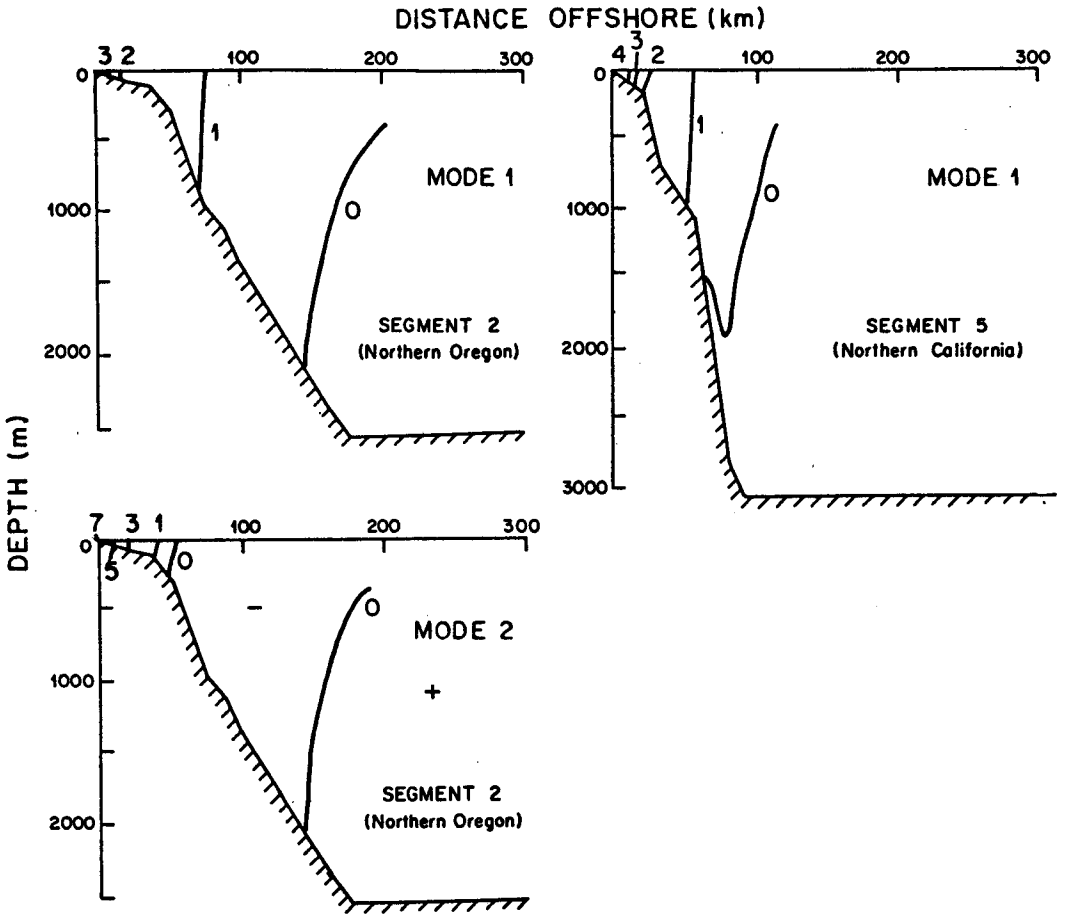

FIG. 5. Offshore-vertical structure of modeled nondimensional longshore velocity for the mode one and mode two hybrid waves in segment 2 (northern Oregon) and for the mode one wave in segment 5 (northern California).

The density profile was assumed invariant in the cross-shelf direction for the dispersion curve and model structure calculations. In the upper layer (0–200 m), isopycnals can substantially deviate from the horizontal position. The demonstrated insensitivity of the results to large variations in near-surface stratification suggests that the approximation $N(x, z) \approx N(z)$ is not a significant source of error at low (nondispersive) frequencies.

The calculations along the remaining coastal segments gave results similar to those off Oregon; specifically, a nondispersive frequency range where the modal structure and phase speed are not significantly affected by seasonal changes in stratification (not

TABLE 2. Properties of the first mode wave for different west coast segments: c_1 is the mode one phase speed, b_1 the mode one wind coupling coefficient, T_F the frictional decay time, and $\Delta\xi$ the length of the coastal segment. W is the cumulative effect of friction given by $W = \exp(\int_0^y a_1 d\xi)$, where a_1^{-1} is the frictional decay length for mode one ($a_1^{-1} = c_1 T_F$).

	Segment							
Property	1	2	3	4	5	6	7	8
c_1 (m s^{-1})	4.8	4.8	3.8	3.2	3.0	2.8	2.8	2.8
$b_1 \times 10^2$ (cm$^{-1/2}$)	0.80	0.80	0.72	0.65	0.68	0.68	0.68	0.68
T_F (days)	9.0	9.0	9.0	10.0	10.0	11.0	12.0	13.0
$\Delta\xi$ (km)	220	220	150	300	380	450	510	150
W (Neah Bay)	0.94	0.89	0.84	0.76	0.65	0.55	0.46	0.44
W (South Beach)	—	—	0.96	0.86	0.74	0.63	0.51	0.49

shown), and a response that is highly barotropic (Fig. 5). The variation of phase speed along the coast for mode one is illustrated in Table 2.

b. *Wind-forced coastal trapped wave model*

Clarke (1977) showed that it is possible to model coastal sea level and current response to wind forcing for the case of long ($\partial_{tt}^2 \ll f^2$ and $\partial_{yy}^2 \gg \partial_{xx}^2$) waves. The long waves are nondispersive so that the model is limited to the low-frequency band ($\leq$0.3 cpd). The pressure field is first expanded into an infinite orthogonal set of free wave modes

$$P(x, y, z, t) = \sum_{n=0}^{\infty} F_n(x, z)\phi_n(y, t), \qquad (2.12)$$

where each mode, when excited by a longshore wind stress τ, is governed by the following equation:

$$\phi_{ny} + c_n^{-1}\phi_{nt} + a_n\phi_n = b_n\tau. \qquad (2.13)$$

In (2.12) and (2.13) F_n describes the offshore-vertical structure of the free wave mode with phase speed c_n, a_n is the friction damping coefficient, b_n the wind coupling coefficient, and τ the longshore component of wind stress, assumed constant in the x direction. For details of the development of equations (2.12) and (2.13) see Clarke (1977) and Brink (1982a).

Brink (1982b) provides a method for estimating the contribution of bottom friction to a_n. The calculation involves root mean square velocity averaged over the offshore extent of the wave. A value of 20 cm s^{-1} was used in segments 1–4 (from data off Washington in Smith *et al.*, 1976); a value of 15 cm s^{-1} was used in segments 5–8. A lower value was used off California, where the shelf width is less, to account for the fact that a higher percentage of the wave occurs over a lower velocity region.

If the frictional decay length a_n^{-1} is much larger than a characteristic wave length, Eq. (2.13) can be integrated by the method of characteristics to give

$$\phi_n(0, t) = \phi_n\left(y, t - \int_0^y c_n^{-1}d\xi\right)\exp\left(-\int_0^y a_n d\xi\right) + \int_0^y b_n(\xi)\tau\left(\xi, t - \int_\xi^y c_n^{-1}d\xi'\right)\exp\left(-\int_\xi^y a_n d\xi'\right)d\xi, \qquad (2.14)$$

where $\xi = y$ ($y < 0$), and y is the starting point of the calculation (on the west coast of the United States, y is equatorward of the point $y = 0$). The first term in equation (2.14) describes a coastal trapped wave propagating freely along the coast ($c_n > 0$) modified by friction. The second term describes the response of the wave amplitude function ϕ_n to past ($t < 0$) forcing along the wave's path to ($y = 0$, $t = 0$), reduced in magnitude by friction encountered en route to $y = 0$. Note that since the wave energy can propagate only in the direction of increasing y (i.e., northward along this coast), the response at a given location is only influenced by winds south of that location.

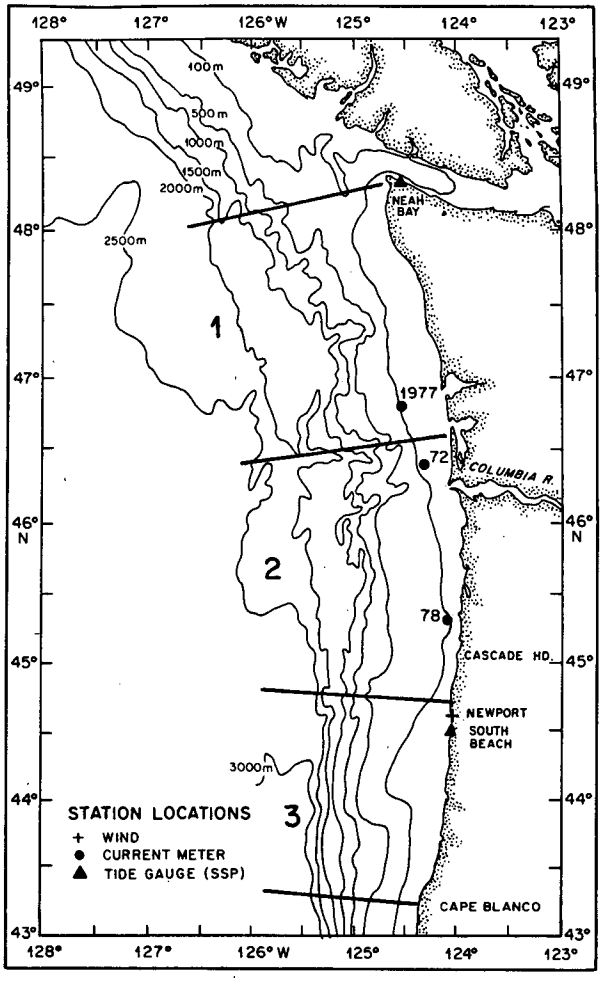

FIG. 6. Topographic map and locations of current meter, wind and SSP stations for the Pacific Northwest. Segments for the coastal trapped wave model are indicated as lines emanating from the coast.

It is assumed that the first mode dominates the response in the pressure field and hence the infinite sum in (2.12) is replaced by the mode one coastal trapped wave ($n = 1$) (see Clarke, 1977; Brink, 1982a).

3. Comparisons between theory and observation

The integration in Eq. (2.14) was performed over the eight segments depicted in Fig. 1. The calculated values of c_1, b_1, and $T_F = (c_1 a_1)^{-1}$ for each segment are listed in Table 2. Phase speed increases significantly toward the north, particularly off the northern Oregon and Washington coasts, primarily due to the gradually increasing shelf width toward the north. The northward increase in shelf width is also responsible for the northward increase in the importance of bottom friction and for the northward increase in magnitude of the wind coupling coefficient b_1. Note that the wave decay

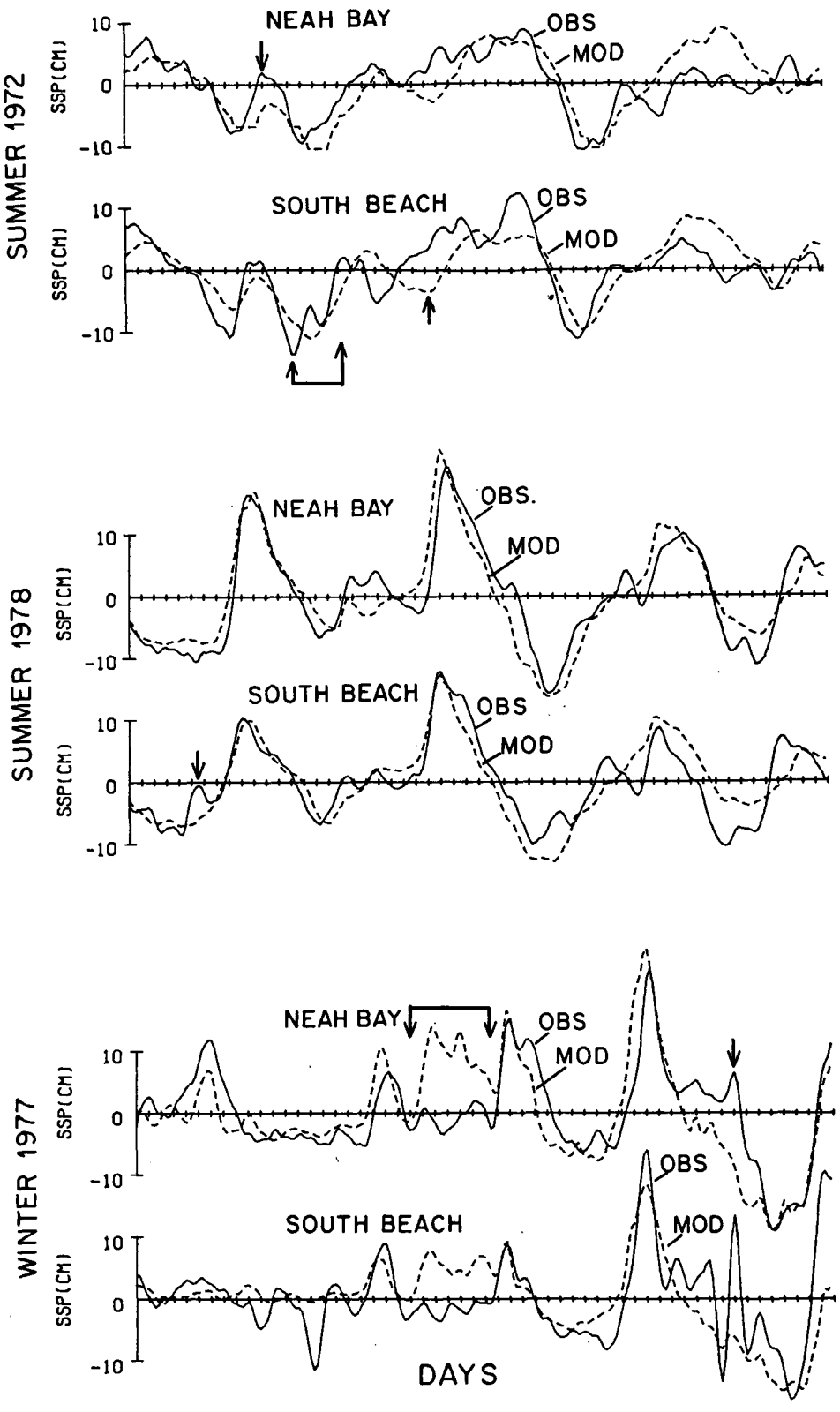

FIG. 7. Observed (OBS) and modeled (MOD) subsurface pressure (SSP) for Neah Bay, Washington and South Beach, Oregon during 21 July–15 September 1972, 15 August–15 October 1978 and 12 January–5 March 1977. Each tick on the time axis represents one day. Vertical arrows correspond to those in Fig. 16 (see text).

TABLE 3. The percentage of variance in coastal subsurface pressure at Neah Bay (NB), Washington and South Beach (SB), Oregon contributed by each segment (per unit segment length) in summers 1972 and 1978 and winter 1977. Record length is 56 days in every case. Note that the calculation for SB terminates in segment 3.

	Section							
	1	2	3	4	5	6	7	8
NB 72	3.6	8.3	4.6	12.6	35.8	18.0	14.9	2.2
SB 72	—	—	6.3	15.2	36.4	22.1	18.9	1.1
NB 78	12.9	10.6	6.0	12.2	36.6	8.8	9.4	3.5
SB 78	—	—	9.2	16.8	46.6	12.0	13.4	1.9
NB 77	37.3	27.7	15.3	10.2	3.8	2.1	2.1	1.5
SB 77	—	—	47.5	28.0	10.5	6.2	6.0	1.8

from a signal originating 2400 km south of Neah Bay (1980 km south of South Beach) is significant: only 50% of this signal reaches the point of interest. Since the contribution to the variance of the total pressure off Washington from segment 8 was <5% (see Table 3), this segment was chosen to begin the integration; i.e., in this segment the first term in equation (2.14) could be neglected without significant error.

Ideally, observed wind data would be used in the integration of (2.14). However, a continuous time series of observed winds over such an extensive area is difficult to assemble. Therefore the wind stress coefficients provided by A. Bakun at locations along the coast separated by three degrees of latitude (see Fig. 1) were used in the present calculations. These wind stress data are calculated at 6 h intervals using synoptic surface atmospheric pressure maps, rotating the geostrophic wind vector 15 deg to the left and reducing it by 30% to include frictional effects (Bakun, 1975). A spatially averaged wind stress for each coastal segment was obtained by linearly interpolating between Bakun wind

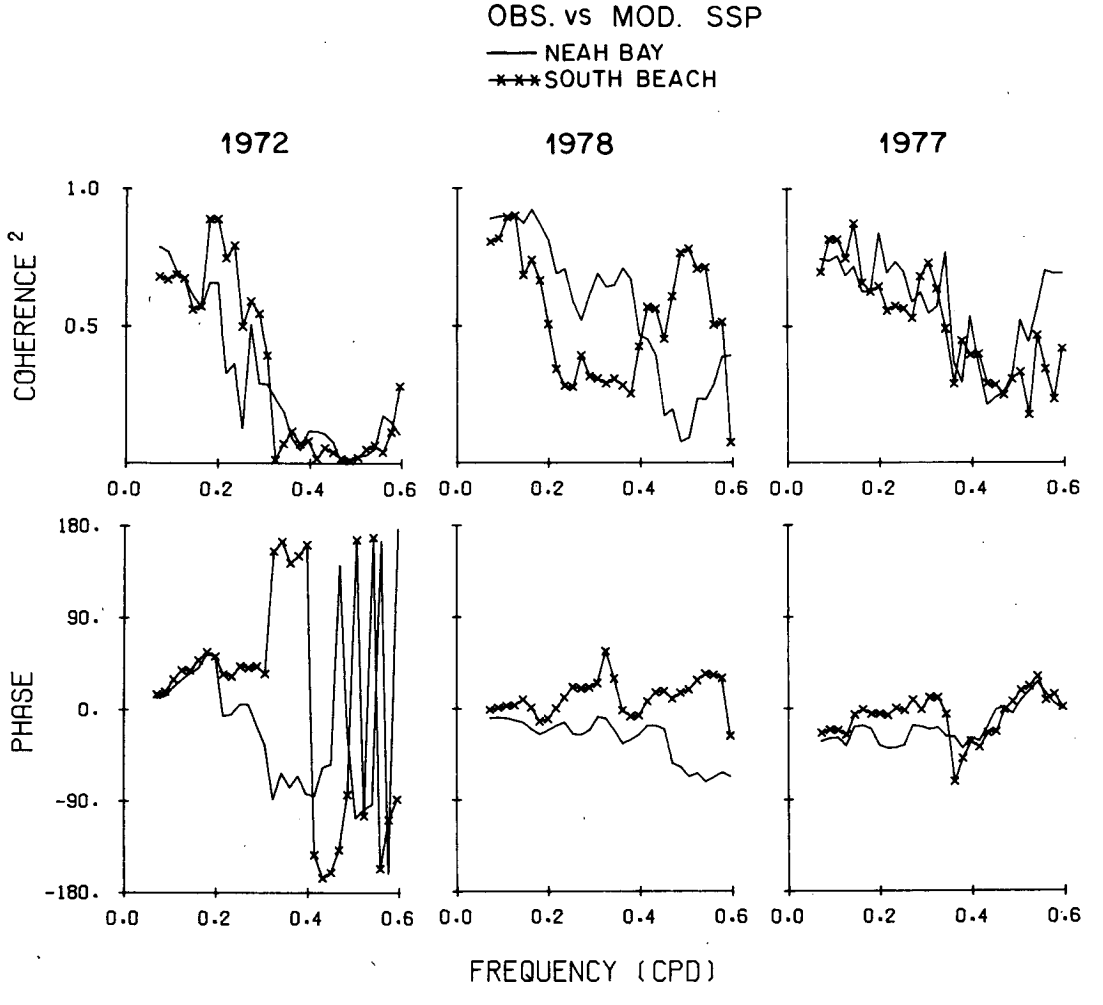

FIG. 8. Coherence squared and phase estimates between observed and modeled subsurface pressure (SSP) at Neah Bay, Washington and South Beach, Oregon in summer 1972, summer 1978 and winter 1977. Each record length is 56 days. A positive phase lag indicates that observed SSP leads modeled SSP. A coherence squared of 0.47 is significant at the 95% level (Koopmans, 1974). Error bars on phase differences are ±24° for a coherence squared estimate that is just significant at the 95% level (Jenkins and Watts, 1968).

stations and averaging the values so obtained within each segment. A discussion of the accuracy of the Bakun wind data is given in Section 4.

The observed subsurface pressure (SSP) records consist of the sum of tide gauge height and atmospheric pressure (converted from mb of pressure to cm of water). These hourly data were filtered with a symmetrical cosine filter whose half power point is 0.6 cpd to remove tidal and inertial frequencies. The data were then decimated to 6 h intervals. The individual raw data sources are described in Hickey (1984). SSP series were generated in this manner for Neah Bay, Washington and South Beach, Oregon. The current meter data were similarly filtered to remove the high frequency signals and decimated to 6 h intervals. These data were also rotated into a local isobath frame of reference. The location of the current meters relative to local topography and relative to the SSP stations are shown in Fig. 6. Data sources are listed in Table 1.

a. Coastal subsurface pressure

The visual similarity between modeled and observed SSP fluctuations at both SSP stations during all three periods is striking (Fig. 7). Coherences between the two series at low frequencies (<0.2 cpd) are significant at the 95% level and are relatively high (0.75–0.95) (Fig. 8). The average phase difference between observed and modeled fluctuations over the low frequency band is within 30° of zero for all cases. The relative lack of coherence at higher frequencies in several cases is noted. However, the majority of the variance (>80%) in the SSP signal is at the lower frequencies, which explains the high visual coherence between the modeled

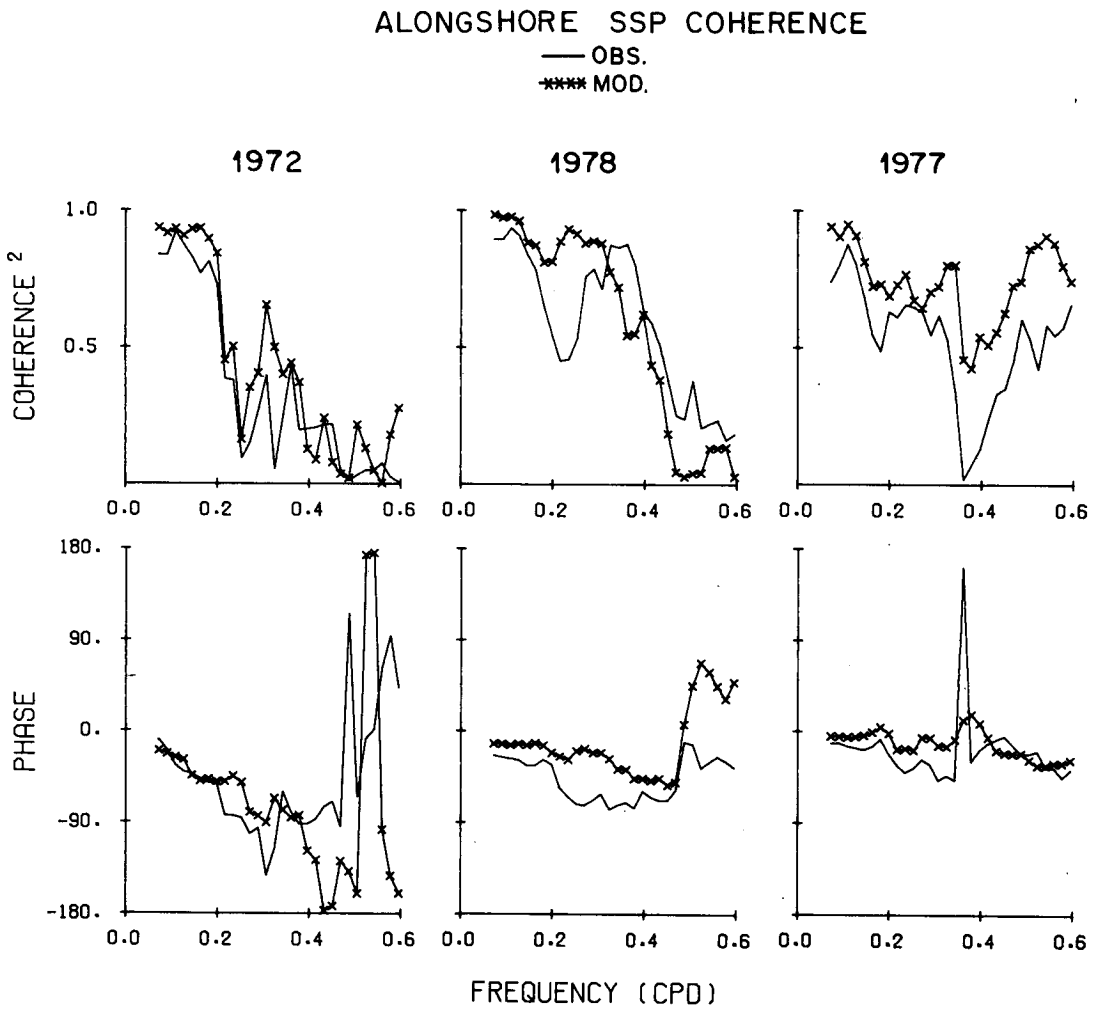

FIG. 9. Modeled and observed coherence squared and phase estimates between SSP at Neah Bay, Washington and that at South Beach, Oregon for summers 1972 and 1978 and winter 1977. Each record length is 56 days. A negative phase difference indicates northward propagation. A coherence squared of 0.47 is significant at the 95% level (Koopmans, 1974). Error bars on phase differences are ±24° for a coherence squared estimate that is just significant at the 95% level (Jenkins and Watts, 1968).

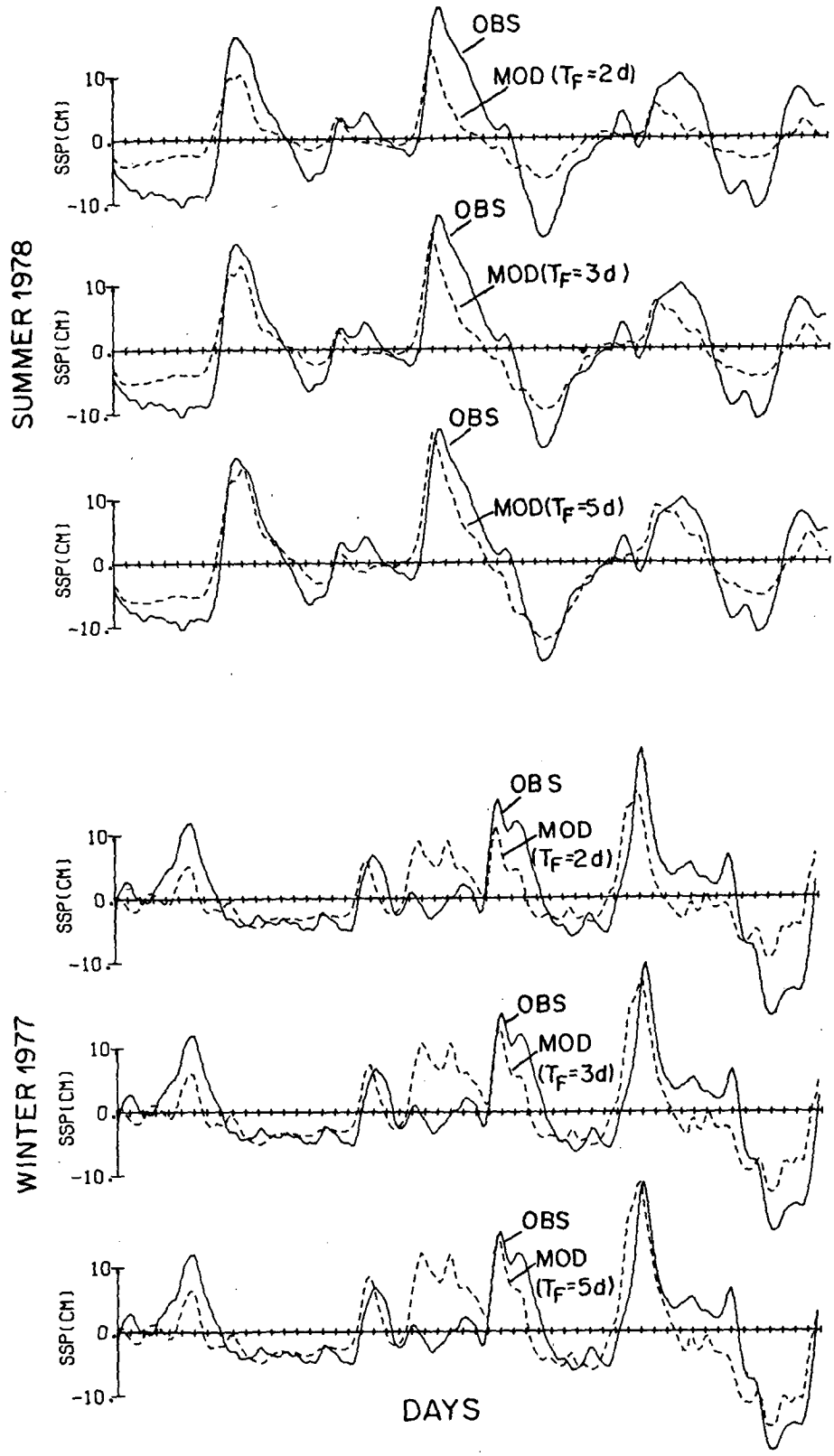

FIG. 10. Modeled (MOD) and observed (OBS) subsurface pressure (SSP) for Neah Bay, Washington in summer 1978 and winter 1977, with model decay time scales (T_F) of 5, 3 and 2 days. Each tick on the time axis represents one day.

and observed series. The observed phase speeds between South Beach and Neah Bay averaged over the low frequency band are on the order of 500, 900, and 1600 km d^{-1} for 1972, 1978 and 1977; modeled phase speeds are on the order of 510, 1600, and >3000 km d^{-1}, respectively (Fig. 9).

To evaluate the sensitivity of the forced wave model to the parameterization of bottom friction, the calculations were repeated for Neah Bay 1978 and Neah Bay 1977 for frictional decay times of 5, 3 and 2 days (Fig. 10). A damping time less than 5 days clearly underestimates the magnitude of the SSP response for both cases. The phase of the SSP response is not extremely sensitive to the choice of decay times. For summer 1978, the phase difference between the observations and the model was on the order of ten degrees closer to zero with the five day than with the two day decay time. For winter 1977 the phase difference was only five degrees. Results for the summer 1972 data are similar to that in summer 1978 (not shown).

In order to identify regions of significant contribution to the variance in coastal SSP in the Pacific Northwest, variance along each coastal segment was calculated from the model for each of the cases depicted in Fig. 7 (Table 3). The variance from each segment for the entire record length was normalized to the length of coast in that segment. For both summer cases the majority of the variance in coastal SSP (>35%) is *remotely* generated between Cape Mendocino and San Francisco, California—a distance of 900–1300 km south of Neah Bay. Since the wind coupling coefficients differ only slightly along the coast (in fact they favor the locally forced response), the enhanced wave generation along this segment compared to that farther north is primarily a reflection of the relatively energetic wind forcing along this segment during summer. Wind stress spectra show that, for both summer cases, the winds at 39°N are more energetic than those both to the north or south at the lowest (and most energetic) frequencies (Fig. 11). The longshore structure of wind fluctuations in 1972 is more representative of typical summer conditions than that in 1978 (e.g., see Bakun, 1975).

To determine to what extent the signal generated in the Cape Mendocino/San Francisco segment 5 is masked by the response generated at other locations, the component of the pressure signal at Neah Bay due to segment 1 and that due to segment 5 were plotted individually with the observed pressure at Neah Bay (Fig. 12). It is clear that in summer a significant percentage of the signal is generated by wind forcing off northern California and propagates up the coast to the Pacific Northwest as an unforced propagating coastal trapped wave. In winter 1977 the majority of the variance in SSP was generated more locally than in the summer cases (Fig. 12 and Table 3). Greater than 70%

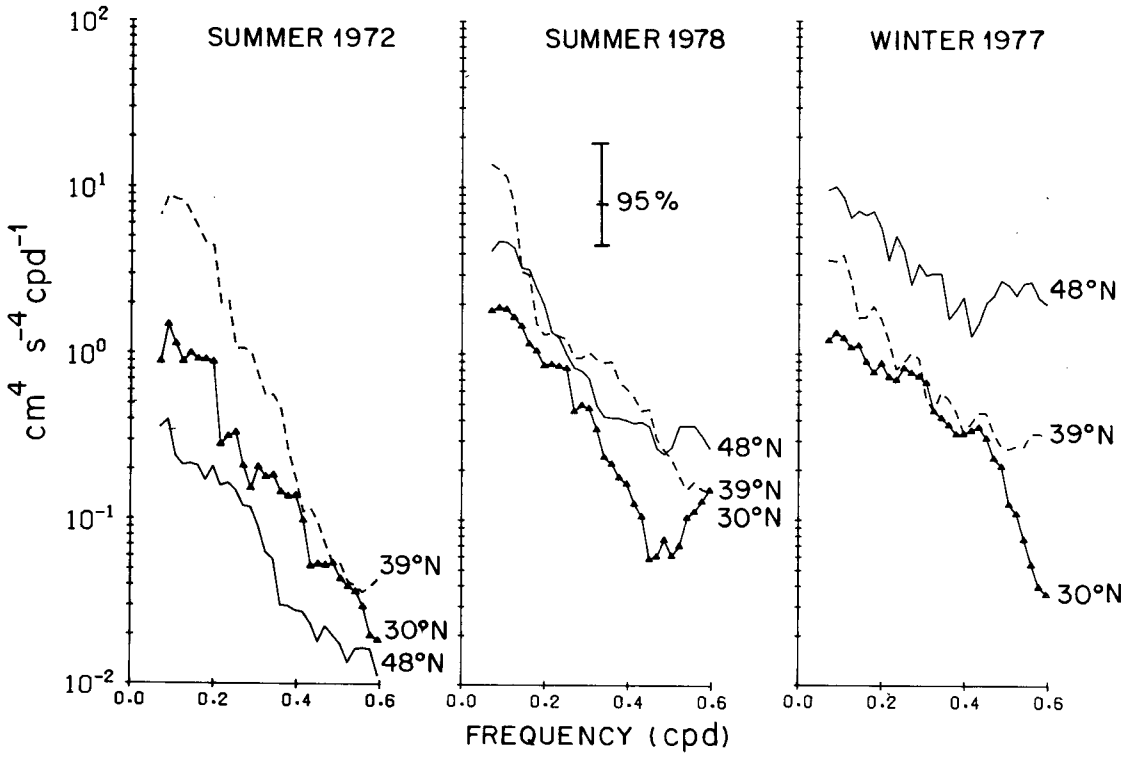

FIG. 11. Spectra of wind stress as a function of latitude in summers 1972 and 1978 and winter 1977. Each record length is 56 days. Confidence limits were derived from Koopmans (1974).

of the variance in modeled SSP was generated by wind forcing less than 600 km from the observation location at both Neah Bay and South Beach, consistent with the northward increase in wind stress variance that occurs along the coast during winter (Fig. 11).

b. The low frequency velocity field

Brink (1982a) used remote wind-forced coastal trapped wave theory to model the observed velocity field off the coast of Peru: the study was only marginally successful, apparently due to the quality of the wind data set. Empirical orthogonal eigenfunction analysis of longshore velocity data off Washington during summer 1972 suggests at least qualitative consistency with the mode one wave structure (Fig. 13 versus Fig. 5): an amplitude that decays offshore, quasi-barotropic velocity profiles and no zero crossing over the shelf–slope region. Eq. (2.1) for the free coastal trapped wave in the nondispersive frequency band gives

$$v = \frac{P_x}{\rho_0 f}, \tag{3.1}$$

i.e., the longshore currents are geostrophic over the shelf. This relationship was used to model the velocity field at midshelf, the shelf edge and also over the slope. The results for mid-water column, midshelf currents (bottom depths of 78, 110 and 100 m in 1972, 1978 and 1977, respectively) are shown in Fig. 14. The moorings are roughly 20, 15 and 40 km from shore in the three cases (Fig. 6). For the summer cases, mod-

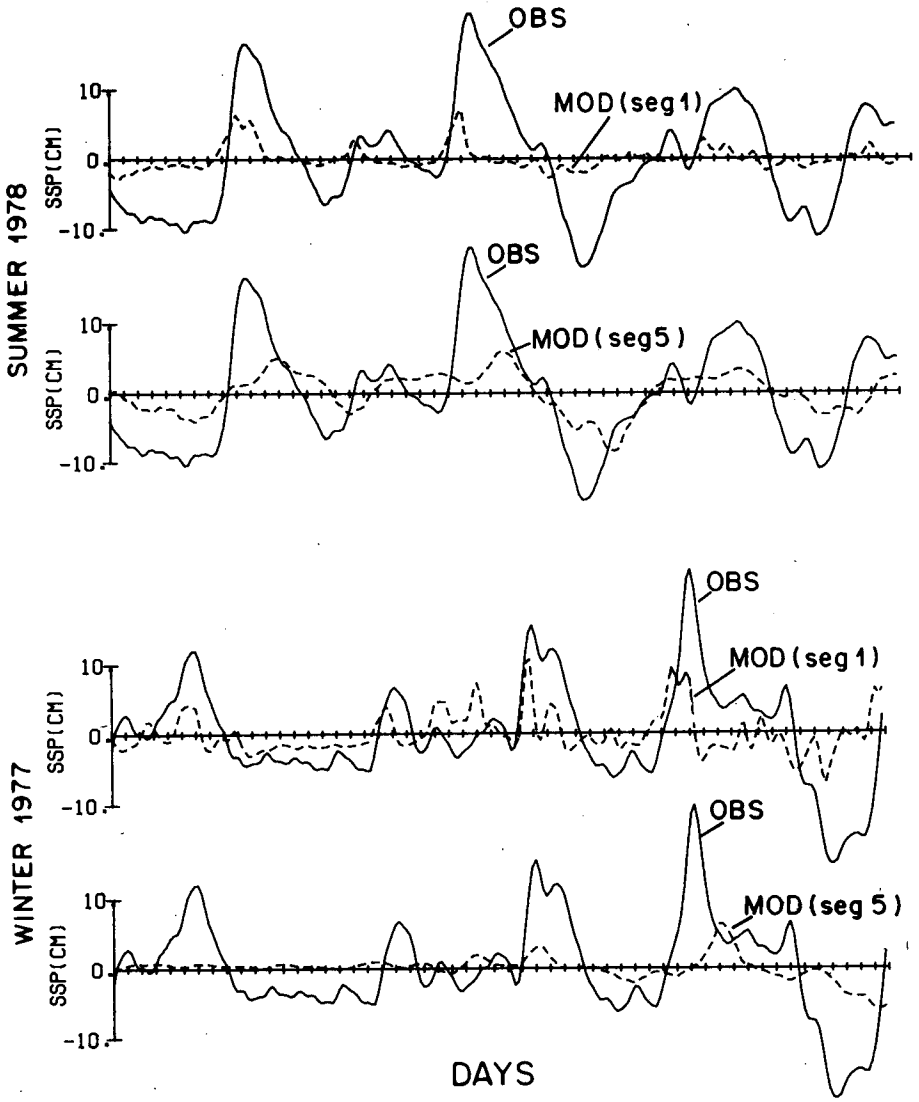

FIG. 12. Subsurface pressure (SSP) modeled by the freely propagating mode one coastal trapped wave forced by local winds (segment 1) and by winds off northern California (segment 5) versus observed SSP for Neah Bay in summer 1978 and winter 1977. Each tick on the time axis represents one day.

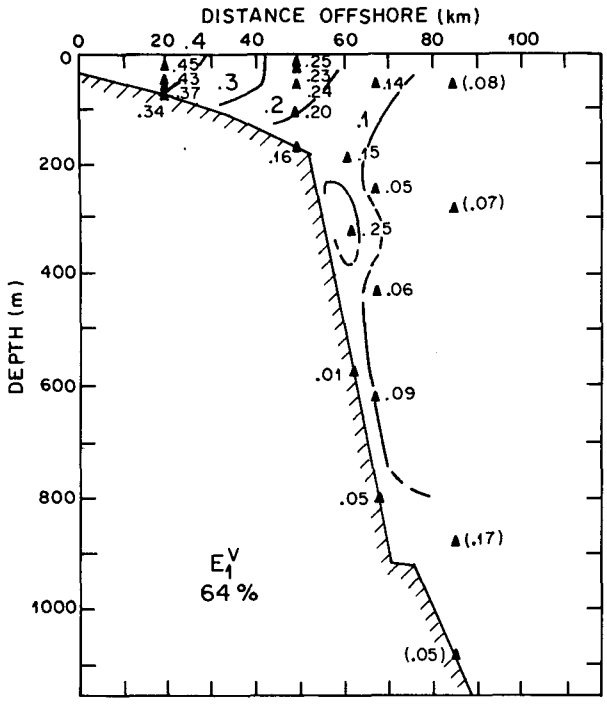

FIG. 13. Amplitude of the first empirical orthogonal eigenfunction E_1^v of observed longshore velocity off Washington in summer 1972, for the period 21 July–26 August. Numbers in brackets were calculated for the shorter period 21 July–16 August. Note that contours have been drawn excluding data in the expected bottom frictional layer (~15 m) on the shelf, i.e., the modal structure over the shelf does appear to have a small baroclinic component. Depths of current meters are indicated by triangles. Mooring locations are listed in Table 1. The first empirical orthogonal function accounts for 64% of the total variance.

eled velocity agrees reasonably with observed velocity in shape, phase and magnitude, although the magnitude of the modeled velocity is significantly lower than that observed in 1972. The modeled and observed velocity fluctuations during both summers are significantly coherent at frequencies $\leq$ 0.2 cpd (Fig. 15). During summer 1978 the coherence is particularly high (>0.85) and the phase difference between modeled and observed velocity is less than 20°. The structure of the coherence spectrum is markedly different during winter 1977 from that during the two summers: coherence over most of the low frequency band (<0.2 cpd) is not significant at the 95% level and coherence at higher frequencies is significant across a much broader frequency range than during summer.

To explore the accuracy of model predictions for the velocity field farther offshore, additional coherence estimates between observed and modeled longshore velocity fields were made for mid-water column data in summer 1972 at NH20 (50 m; 35 km offshore; bottom depth 150 m) and at several of the mooring locations used in the EOF of Fig. 13: OS (30 and 50 m; 50 km offshore; bottom depth 170 m), S6 (192 m; 62 km offshore; bottom depth 597 m) and S8 (60 m; 66 km offshore; bottom depth 818 m). Coherences at low frequencies were significant at the 95% level at all depths tested with an average phase difference in the low frequency band of <25°.

4. Discussion

The most significant source of error in modeling the low frequency coastal response in SSP and longshore velocity is the use of Bakun winds instead of observed coastal winds. Bakun winds are computed from atmospheric pressure differences and are, at best, a representation of the large-scale (>300 km) wind field. The difference between Bakun wind stress at 45°N and Newport wind stress for all three periods is illustrated in Fig. 16. The Newport wind station, which is maintained by Oregon State University, has good exposure (Pittock *et al.*, 1982) and has been compared favourably with *in situ* wind measurements (Halpern, 1976). The *in situ* measurements suggest that midshelf stress is a factor of about 1.7 larger than that at Newport during summer (Hickey, 1984), which may account for some of the observed Bakun-Newport magnitude differences in winter 1977 and in summer 1978, but not in summer 1972. When this offshore increase in wind stress is included, it is apparent that summer 1972 Bakun wind data are much less energetic than local winds. In addition, the coherence between Bakun and Newport wind stress in the band 0.10–0.15 cpd is not significant at the 95% level (r^2 = 0.2) during summer 1972.

The fact that in spite of major discrepancies between local and Bakun winds, the first mode CTW calculated using Bakun wind data seems to model the coastal SSP adequately in both amplitude and phase much of the time, substantiates the integration nature of the forced wave response. During summer, when the primary generation region for the fluctuating SSP in the Pacific Northwest is off northern California, inaccuracies in the prescription of the local wind field are relatively unimportant. During winter, on the other hand, when more local wind stress accounts for the majority of SSP variance in the Pacific Northwest, an accurate prescription of the local wind field is much more important. Comparison of Fig. 7 with Fig. 16 illustrates that during winter 1977, several major differences between the modeled and observed SSP occurred during periods of major difference in local and Bakun wind stress data. Examples are indicated in the two figures with vertical arrows. This is also the case in summer 1972, which may account for the relatively poor (cf., 1978) model predictions, including an underprediction of amplitude (see Figs. 7 and 8). Hickey (1984) uses the local Newport wind data to describe summer 1972 as a case of strong local wind forcing (of longshore current acceleration fluctuations) and summer 1978 as a case of very weak local wind forcing. It is clear from Fig. 16 that the large-scale Bakun wind

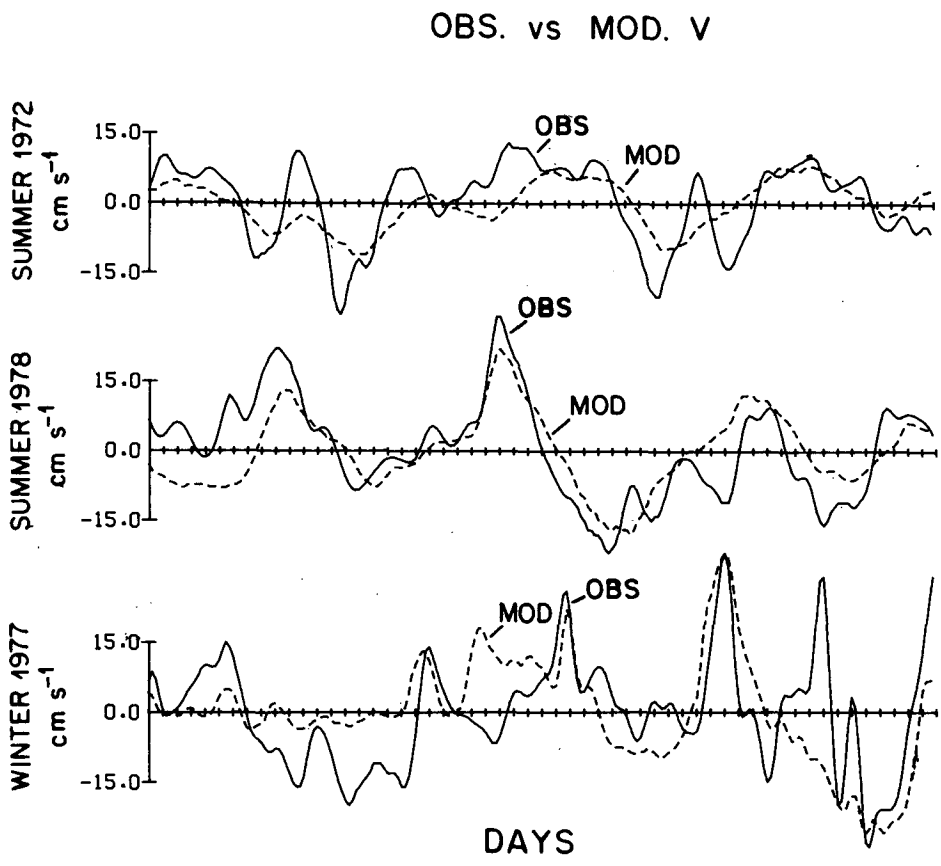

FIG. 14. Observed (OBS) and modeled (MOD) longshore velocity for mid-water column, midshelf locations in summers 1972 and 1978 and winter 1977. Each tick on the time axis represents one day.

data give quite the opposite result. The perhaps spuriously large Bakun wind stress in 1978 could be responsible also for the fact that the model predicts a faster than observed SSP phase speed during that period, i.e., the observations may be more free-wave like than the model predicts.

The wind coupling coefficients b_1 and the frictional decay times T_F ($\sim$10 days) used in the forced wave integration (2.14) were obtained theoretically. Sensitivity analysis also suggested that a time scale between 5 and 10 days provided the best amplitude and phase fit to the three sets of observations. Halliwell and Allen (1984) present a forced wave calculation off the west coast of the United States for a period during summer, 1973. They estimated both b_1 and T_F by finding the best fit between calculated and observed SSP. The resulting longshore averaged T_F was on the order of 4 days, a factor of two less than the theoretical value used herein. As in the present study, this estimate was relatively insensitive to significantly larger decay times. The precise value of T_F cannot easily be determined with available data sets. It should be stressed that in spite of these differences, both studies give similar estimates of the contribution of remote wind forcing to coastal SSP in the Pacific Northwest during summer.

5. Conclusion

The remotely wind forced coastal trapped wave model of Clarke (1977) is applied to the west coast of the United States to model the coastal subsurface pressure (SSP) and longshore velocity fields for three different time periods; 21 July–15 September 1972, 15 August–15 October 1978 and 12 January–5 March 1977. The mode one response is assumed dominant and is used to compare directly with observations during these time periods. Wave characteristics such as phase speed, wind coupling coefficients and frictional decay times were calculated according to Brink (1982b) for each of eight coastal segments from Baja California to Northern California.

Results show that at low frequencies ($\leq$0.2 cpd) the mode one remotely forced coastal trapped wave response in coastal subsurface pressure accurately models the observed SSP in the Pacific Northwest in phase and amplitude for all three cases. The model indicates that during summer, a significant (>35%) amount of

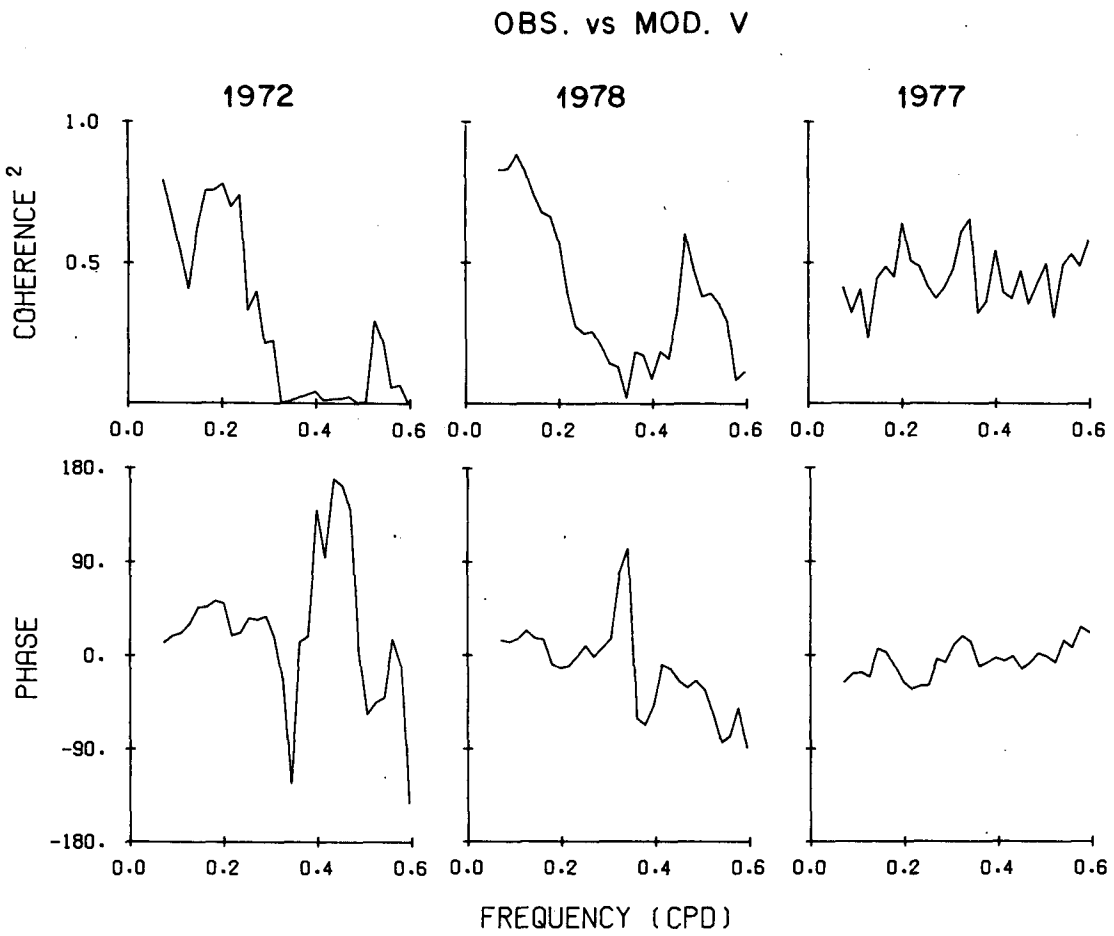

FIG. 15. Coherence squared and phase estimates between observed and modeled longshore velocity records shown in Fig. 14. A positive phase difference indicates that the observed velocity leads the modeled. Each record length is 56 days. A coherence of 0.47 is significant at the 95% level (Koopmans, 1974). Error bars on phase differences are ±24° for a coherence squared estimate that is just significant at the 95% level (Jenkins and Watts, 1968).

the variance in SSP off Oregon and Washington is generated by wind forcing between San Francisco and Cape Mendocino, California. The signal propagates northward ~900–1300 km to Washington–Oregon as a frictionally damped mode one CTW, arriving 3 to 4 days later. During winter, the most significant contribution to the variance in SSP at low frequencies off Washington and Oregon is generated more locally (<600 km south of the observing station). The seasonal difference is due to seasonal differences in the large scale wind field which has significantly higher (lower) winds between 42–48°N than farther south during the winter (summer) months.

Model calculations of the mode one longshore velocity were also significantly coherent with observed longshore velocity fluctuations across the low frequency band (<0.2 cpd) during summer. During winter, coherence in the low frequency band was much reduced in comparison to the summer situation.

Comparison between local coastal wind data and the Bakun data which were used to model the mode one response suggests that many of the differences between the modeled and observed SSP are a result of inadequate prescription of the wind forcing. This is particularly true during winter when a majority of the wind forcing is local to the Pacific Northwest. Thus a more realistic simulation of wind forced wave generation would be one that included local wind data for some distance south of the location being examined. The authors note that this approach, while seemingly straightforward, opens the proverbial "can of worms" concerning not only measured and computed (Bakun) winds, but also measured coastal winds and measured "over-water" winds. Unless the transfer function between these wind datasets is known, it is difficult, to say the least, to perform valid model calculations with such a "mixed" dataset. The authors consequently leave this analysis to future study.

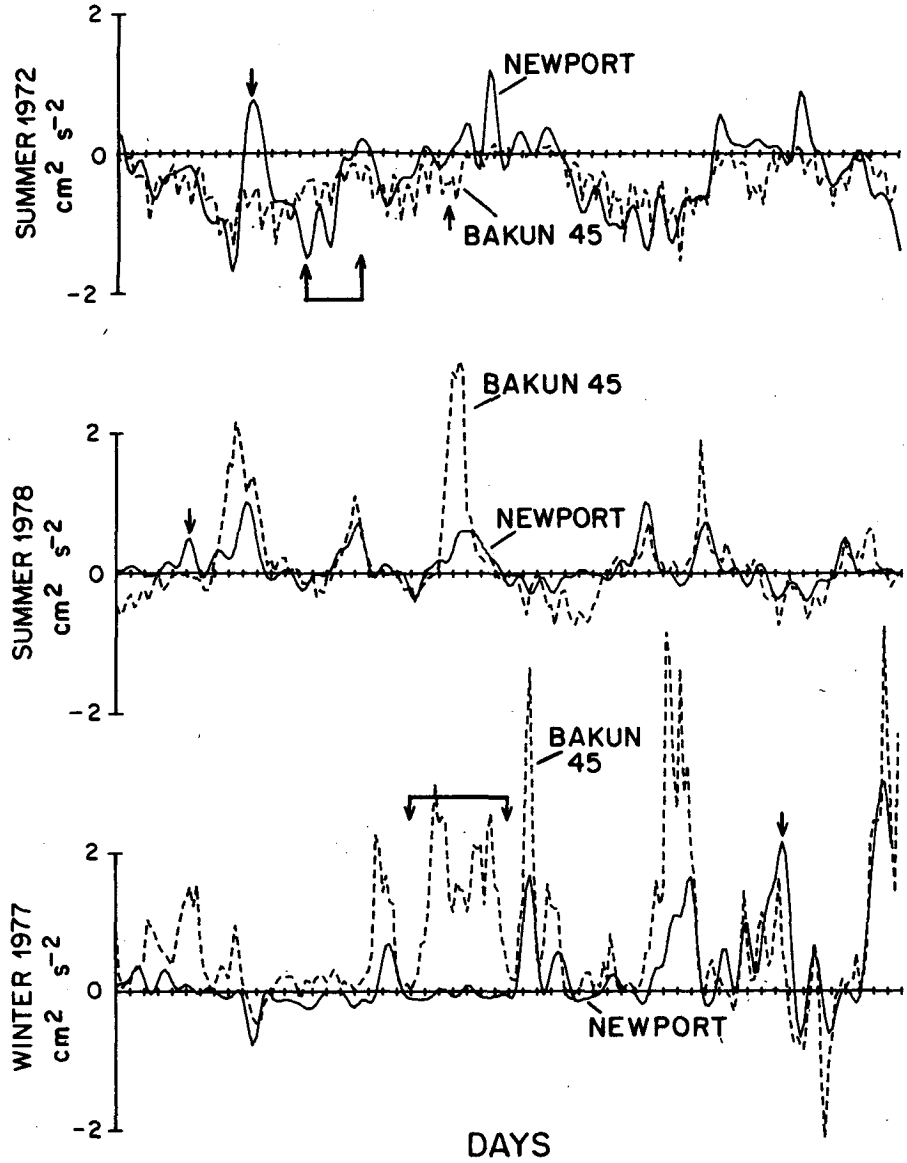

FIG. 16. Wind stress from a local coastal station (Newport) versus Bakun wind stress computed at 45°N in summers 1972 and 1978 and winter 1977. Relative station locations are shown in Fig. 1. Wind stress at Newport was computed from hourly data using a constant drag coefficient of 1.3 $\times 10^{-3}$. Vertical arrows indicate examples of relatively large differences between the two stress estimates that appeared to degrade the accuracy of the model (see corresponding arrows in Fig. 7).

Acknowledgments. The authors would like to thank Dr. Ken Brink for supplying the numerical wave model, Dr. A. Bakun for supplying coastal wind stress data, and Drs. A. Huyer and R. L. Smith for supplying Newport wind data and NH20 current meter data. A special thanks is extended to Susan Geier, who was responsible for the majority of the computer graphics. This analysis was supported by the National Science Foundation under Grants OCE 80-23465 and OCE 83-08196 and by the Department of Energy under Contract DE-AT06-76-EV-71025.

REFERENCES

Adams, J. K. and Buchwald, V. T., 1969: The generation of continental shelf waves. *J. Fluid Mech.*, **35**, 815–826.

Allen, J. S., 1975: Coastal trapped waves in a stratified ocean. *J. Phys. Oceanogr.*, **5**, 300–325.

Bakun, A., 1975: Daily and weekly upwelling indices, west coast of North America, 1967–1973. NOAA Tech. Rep., NMFS SSRF-93, 114 pp.

Brink, K. H., 1982a: A comparison of long coastal trapped wave theory with observations off Peru. *J. Phys. Oceanogr.*, **12**, 897–913.

——, 1982b: The effect of bottom friction on low-frequency coastal trapped waves. *J. Phys. Oceanogr.*, **12**, 127–133.

Clarke, A. J., 1977: Observation and numerical evidence for wind-forced coastal trapped long waves. *J. Phys. Oceanogr.*, **7**, 231–247.

——, and D. S. Battisti, 1983: Identification of the fortnightly wave observed off the northern coast of the Gulf of Guinea. *J. Phys. Oceanogr.*, **13**, 2192–2200.

Cutchin, D. L., and R. L. Smith, 1973: Continental shelf waves: low-frequency variations in sea level and currents over the Oregon continental shelf. *J. Phys. Oceanogr.*, **3**, 73–82.

Fleischbein, J., and A. Huyer, 1982: Hydrographic data from a large scale west coast shelf experiment and the Low Level Waste Ocean Disposal Program: R/V *Wecoma* Cruise W8108B, 24 August–6 September 1981. Data Rep. 96, School of Oceanogr., Oregon State University. 62 pp.

——, W. E. Gilbert, A. Huyer and R. L. Smith, 1982: CTD observations off Oregon and California: R/V *Wecoma* W8LL2A-B, 4–16 December 1981. Data Rep. 99, School of Oceanogr., Oregon State University. 80 pp.

Gilbert, W. E., J. Fleischbein, A. Huyer and R. Schramm, 1982: Hydrographic data from the First Coastal Ocean Dynamics Experiment: R/V *Wecoma*, Leg 5, 16–29 May 1981. Data Rep. 93, School of Oceanogr., Oregon State University. 177 pp.

Gill, A. E., and A. J. Clarke, 1974: Wind-induced upwelling, coastal currents and sea-level changes. *Deep-Sea Res.*, **21**, 325–345.

——, and E. H. Schumann, 1974: The generation of long shelf waves by the wind. *J. Phys. Oceanogr.*, **4**, 83–90.

Halpern, D., 1976: Measurements of near-surface wind stress over an upwelling region near the Oregon coast. *J. Phys. Oceanogr.*, **6**, 108–112.

Halliwell, G. R., and J. S. Allen, 1984: Large scale sea level response to atmospheric forcing along the west coast of North America, summer, 1973. *J. Phys. Oceanogr.*, **14**, 864–886.

Hickey, B. M., 1984: The fluctuating longshore pressure gradient on the Pacific Northwest shelf: A dynamical analysis. *J. Phys. Oceanogr.*, **14**, 276–293.

Hseuh, Y., and C. Lee, 1978: A hindcast of barotropic response over the Oregon-Washington continental shelf during the summer of 1972. *J. Phys. Oceanogr.*, **8**, 799–810.

Hsieh, W. W., 1982: Observations of continental shelf waves off Oregon and Washington. *J. Phys. Oceanogr.*, **12**, 887–896.

Huthnance, J. M., 1978: On coastal trapped waves: Analysis and numerical calculations by inverse iteration. *J. Phys. Oceanogr.*, **8**, 74–92.

Huyer, A., B. M. Hickey, J. D. Smith, R. L. Smith and R. D. Pillsbury, 1975: Alongshore coherence at low frequencies in currents observed over the continental shelf off Oregon and Washington. *J. Geophys. Res.*, **80**, 3495–3505.

Jenkins, G. M., and D. G. Watts, 1968: *Spectral Analysis and its Applications*. Holden-Day, 525 pp.

Koopmans, L. H., 1974: *The Spectral Analysis of Time Series*. Academic Press, 336 pp.

Kundu, P. K., and J. S. Allen, 1976: Some three-dimensional characteristics of low-frequency current fluctuations near the Oregon coast. *J. Phys. Oceanogr.*, **6**, 181–199.

——, J. S. Allen and R. L. Smith, 1975: Modal decomposition of the velocity field near the Oregon coast. *J. Phys. Oceanogr.*, **5**, 683–704.

Mooers, C. N. K., and R. L. Smith, 1968: Continental shelf waves off Oregon. *J. Geophys. Res.*, **73**, 549–557.

Pittock, H. L., W. E. Gilbert, A. Huyer and R. L. Smith, 1982: Observations of sea level, wind and atmospheric pressure at Newport, Oregon, 1967–1980. NSF Data Rep. 98, 158 pp.

Smith, J. D., B. M. Hickey and J. Beck, 1976: Observations from moored current meters on the Washington continental shelf from February 1972–February 1974. Dept. of Oceanogr. Special Rep. No. 65, University of Washington, 383 pp.

Wang, D. P., and C. N. K. Mooers, 1977: Coastal trapped waves in a continuously stratified ocean. *J. Phys. Oceanogr.*, **6**, 853–863.